ARTICLE IN PRESS

Available online at www.sciencedirect.com

ScienceDirect

ELSEVIER

International Journal of Impact Engineering ▮ (▮▮▮▮) ▮▮▮–▮▮▮

INTERNATIONAL JOURNAL OF IMPACT ENGINEERING

www.elsevier.com/locate/ijimpeng

Protection performance of dual flying oblique plates against a yawed long-rod penetrator

S.H. Paik[a], S.J. Kim[b,*], Y.H. Yoo[c], M. Lee[d]

[a]*School of Mechanical and Aerospace Engineering, Seoul National University, Seoul 151-742, Republic of Korea*
[b]*School of Mechanical and Aerospace Engineering, Flight Vehicle Research Center, Seoul National University, Seoul 151-742, Republic of Korea*
[c]*Ground System Development Center, Agency for Defense Development, P.O. Box 35-1, Daejeon 305-600, Republic of Korea*
[d]*School of Mechanical and Aerospace Engineering, Sejong University, Seoul 143-747, Republic of Korea*

Received 21 July 2005; received in revised form 10 March 2006; accepted 16 June 2006

Abstract

The protection capability of dual flying plates against a yawed long rod of enhanced L/D is evaluated numerically, where L is the length and D is the diameter of the rod. This study is motivated by the fact that the protection performance of dual plate system is governed by the extent of interaction between a yawed long rod and dual flying plates. The simulations are performed using a newly developed dynamic and impact analysis code, IPSAP/Explicit. The long-rods are $L/D = 15$ and 30 with the velocity falling within the ordnance range (1.5 km/s) and hypervelocity range (2.5 km/s) respectively. The yaw angles are -6°, 0°, and $+6^\circ$. The plate velocities are 0.2, 0.3 and 0.5 km/s. Through the simulation results, we find that dual flying plates system is more effective with longer rod due to the elongated disturbance. The protection performance is more effective for the penetrator with $+6^\circ$ of yaw angle than that with a yaw angle of -6°.

Keywords: Dual flying plate; Hypervelocity; Yawed long-rod; Penetration; Armor effectiveness

1. Introduction

The double flying plates with an explosive between the plates were considered in explosive reactive armor systems [1–3]. Historically, the concept of the reactive armor was first introduced from the defeat of shaped charge jet and a number of experimental [2] and analytical [3] researches on the interaction between jet and flying plates have been performed.

Meanwhile, the protection capability of a stationary (or moving) oblique plate has also been tested with long rod penetrators. For single oblique plate, some of the results from the reverse impact tests with a stationary oblique penetrator were compared with the theoretical results [4,5]. Recently, it was reported that a single plate with obliquity of 60–70° that is moving away from the projectiles at velocities of 0.2 and 0.3 km/s has large disturbing effects causing extensive fragmentation of the projectile [6,7]. It has been found by numerical simulations that an increase in the velocity of oblique plate moving in its normal direction with a

*Corresponding author. Tel: +82 2 880 7388; fax: +82 2 887 2662.
E-mail address: sjkim@snu.ac.kr (S.J. Kim).

0734-743X/$ - see front matter © 2006 Published by Elsevier Ltd.
doi:10.1016/j.ijimpeng.2006.06.006

velocity component towards the incoming penetrator does not necessarily increase the lateral disturbance on the residual penetrator [8]. It also has been reported that, the residual penetration power is inversely proportional to the plate velocity both in the hypervelocity (2.5 km/s) and ordnance velocity (1.5 km/s) impact [9]. Most of these useful informations have already been discussed in the previous works for an obliquely impacting long rod with single plate.

In contrast, there have not been as many analysis activities on dual flying oblique plates against a long rod, which has also drawn much interest in the areas of sensor-activated and reactive armours. For the dual flying plates system, the oblique plates fly away from each other in the normal direction of the plate. The relative motion of the penetrator and the double flying plates plays an important role in the overall performance of the protection system. In the previous study [10], the effect of weight distribution in dual flying plates on protection capability has been investigated for relatively small L/D long rod without yaw. The backward velocity of a rear plate increases the interaction time with penetrator. Furthermore, the lateral velocity of front and rear plates enlarges the lateral disturbance to the penetrator. Since these effects may be more significant in the longer penetrator, it is expected that dual flying plates system is more effective to the relatively larger L/D penetrator of yaw. These issues are the main focus of the current work. In this study, our purpose is to evaluate the protection capability of dual flying plates system against $L/D = 15$ and 30 penetrator with the ordnance velocity (1.5 km/s) and hypervelocity (2.5 km/s). The effect of the yaw angle and the plate velocity will also be explored.

2. Numerical simulations

2.1. Numerical analysis code

Even though there are several commercial codes that can be used in the simulation of nonlinear dynamic and penetration problems, several laboratories and research groups have developed their own codes for the test of new numerical algorithm and constitutive model. We have also been developing our own parallel explicit dynamic 3-Dim FE code, IPSAP/Explicit (IPSAP: Internet Parallel Structural Analysis Program [11]) for similar reasons. The most important motivation is the need for a parallel code of high parallel efficiency in impact and penetration simulation.

In the IPSAP/Explicit code, one point integration scheme is applied to prevent locking. Spurious modes due to lack of integration points are controlled by hourglass control [12]. The Jaumann rate is used for objective stress update. Velocity, displacement and coordinate are updated with the half step central difference method. The critical time step for stability is determined using the CFL condition. In order to handle the discontinuities in the flow variables associated with shock, artificial bulk viscosity is introduced. For contact treatment, bucket search [13] is used with the exception that bucket size is based on the smallest master surface dimension [14]. In this algorithm, all the buckets occupied by a master surface were collected, after which the slave nodes in those buckets were collected. After gathering a list of potential interaction, a detailed contact check was done for each master segment with the list of slave nodes of potential interaction. This detail contact check determines the best contact pair among the possible candidates, contact point on the master segment, normal vector at the contact point and distance between slave node and contact point. Contact force is determined based on the penalty method. When the elements are eroded, exterior contact surface should be updated. Among the several algorithms available for determining the exterior of a surface, the algorithm proposed in Ref. [14] is used.

In Lagrangian code, one difficult aspects of modeling rod penetration of moving plates used to be the treatment of the interface between the plate and the lateral surface of the penetrator. However, this is no longer a significant problem since contact stiffness is determined based on the volume and bulk modulus of the element [15] to minimize a possibility of significant source of error and contact instability. Furthermore, a fine mesh resolution causing smaller time step size may reduce the interface instability.

2.2. FE modeling

The schematic view of geometric configuration of the model is shown in Fig. 1. Only half of this geometry was modeled in the three-dimensional problem due to the inherent symmetry. The penetrator is 5 mm in

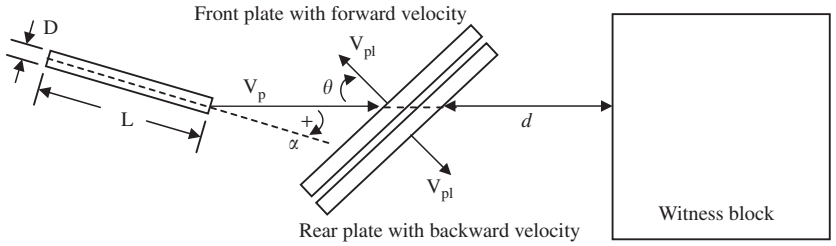

Fig. 1. Schematic view of model.

Table 1
Material constants for Jhonson–Cook model

Material	Density (kg/m^3)	A (Gpa)	B (Gpa)	n	C	m	T_{ref} (K)	T_{melt} (K)
SIS2541-03	7808	0.75	1.15	0.49	0.014	1.0	293	1700
DX2HCMF	17600	1.05	0.177	0.12	0.0275	1.0	293	1723

diameter and 75, 150 mm in length ($L/D = 15$, 30 respectively). The angles of yaw (α) considered are -6°, 0°, and $+6^\circ$. Here, the negative indicates anticlockwise yaw and the positive indicates clockwise yaw. The impact velocity considered are the normal ordnance velocity $V_p = 1.5$ km/s and the hyper velocity regime $V_p = 2.5$ km/s. The plate is 300 mm long and 50 mm wide. Each plate is 2.5 mm in thickness and initial gap between the two plates is 1 mm. The obliquity (θ) of plate is 60°. The plate velocities V_{pl} are 0.2, 0.3 and 0.5 km/s. The witness block is 200 mm high, 50 mm wide, 250 mm long. The initial distance between penetrator and plate is 1 mm and that between plate and witness block ('d' in the Fig. 1) is 240 mm.

In the simulation, the V_p and V_{pl} were set as initial velocities. The penetrator and plates were made to start flying at the initial time such that there is no time interval in the movement between them. Eight elements were modeled along the penetrator diameter and three elements were modeled through the thickness direction of plate. In order to maintain a similar mesh size between the penetrator, plate and witness block, fine mesh with the size of 0.67 mm was modeled around the impact region of the witness block. Therefore, the total number of elements was different depending on the size of fine mesh region of the block. The total number of element is about 200,000–300,000.

In order to consider strain rate hardening as well as thermal softening in addition to the strain hardening considered in static deformation of metallic material, the Johnson–Cook model [16] was used,

$$\sigma = (A + B\varepsilon^n)\left(1 + C\ln\frac{\dot{\varepsilon}}{\dot{\varepsilon}_0}\right)\left[1 - \left(\frac{T - T_{ref}}{T_{melt} - T_{ref}}\right)^m\right]. \quad (1)$$

Here, σ is flow stress, A the static yield strength, B the strain hardening parameter, ε the equivalent plastic strain, n the strain hardening exponent, C the strain rate parameter, $\dot{\varepsilon}$ the equivalent plastic strain rate, $\dot{\varepsilon}_0$ the reference strain rate, T the temperature, T_{ref} the reference temperature, T_{melt} the melting temperature and m the temperature exponent. In this work, the erosion of the finite element is introduced when equivalent plastic strain reaches the value of 1.5. The plate and witness block were modeled with steel (SIS 2541-03) and penetrator was modeled with tungsten heavy alloy (DX2HCMF). The material properties used in the simulation are summarized in Table 1 [8].

3. Numerical result

3.1. Armor effectiveness

Among the several measures of protection capability such as residual length, residual velocity and residual kinetic energy, the armor effectiveness, which is believed to be more realistic and practical measures than the

Table 2
Comparison of reference penetration

Yaw (deg)	V (km/s)	1.5		2.5	
	L/D	15	30	15	30
0	P_N (mm)	61.5	115.2	112.2	207.6
	P_N/L	0.82	0.77	1.48	1.38
	P_N/L	0.83 [19]	0.70 [19]	1.38 [20]	1.33 [20]
6	P (mm)	49.5	71.0	105.7	148.2
	P/P_N	0.80	0.62	0.94	0.71
	P/P_N	—	~0.6 [21]	—	~0.8 [21]

other types, was selected in this work. It is defined as follows:

$$\text{Armor effectiveness } (e) = \frac{P_{\text{ref}} - P_{\text{res}}}{t}, \tag{2}$$

where P_{ref} is the reference depth of penetration (DOP) when a rod with yaw directly hits a witness block, P_{res} is the DOP in the witness block behind the plate by a residual rod, and t is line of sight (LOS) which is the thickness of the oblique plate in the direction of velocity vector of the rod. In this study, LOS was fixed as 10 mm because the thickness of dual plates is 5 mm at 60° obliquity.

Here, we need to examine the definition of P_{ref}, because there may be degradation in P_{ref} for yawed rods. If P_{res} measured by the penetration without yaw is applied to all cases, both oblique plates and yaw angle should be considered in the evaluation of the armor effectiveness at the same time. Hence, the armor effectiveness against yawed rod seems to be more meaningful only if P_{ref} is measured by the penetration with yaw. Table 2 shows a reference penetration including normal and yaw impacts. The predictions agree well with those in the literatures.

3.2. Effect of plate velocity and L/D

The effects of plate velocity and L/D (15 and 30) on the armor effectiveness are presented in Fig. 2. The case of $V_p = 2.5$ km/s is only presented because penetrator with $V_p = 1.5$ km/s cannot penetrate the rear plate but slide on it when V_{pl} is increased to 0.4 or 0.5 km/s. This phenomenon happens for $L/D = 15$ as well as $L/D = 30$ and similar results are found in Ref. [9] for $L/D = 15$. As shown in Fig. 2, the armor effectiveness for $L/D = 30$ shows higher than that for $L/D = 15$. This is due to longer interaction time between the plate and rod. The armor effectiveness increases with increasing plate velocity and the effect of plate velocity is more significant for higher L/D. It seems that the armor effectiveness is slightly higher at positive angle of yaw.

3.3. Effect of yaw angle and impact velocity

The effect of yaw on armor effectiveness is shown in Fig. 3 for the impact velocities of $V_p = 1.5$ and 2.5 km/s. The plate velocities considered are 0.2 and 0.3 km/s. As shown in Fig. 3, the armor effectiveness, in general, is of convex shape and is the highest at zero yaw. This is more prevalent at lower impact velocity. For the case of zero yaw, due to the disturbance of oblique plates the rod has misaligned angle of attack when it impacts the block. For the case of nonzero yaw, however, oblique plates rotate the rod of negative yaw to the positive direction and of positive yaw to the negative direction [17,18], causing the initial angle of yaw to decrease. Hence, the armor effectiveness for the impact of nonzero yaw can be lower than that for of zero yaw. This trend is only true if the reference DOP P_{ref} is evaluated for the direct impact with yaw.

The case of $P_{\text{res}} > P_{\text{ref}}$ is shown in Fig. 3(a) for $L/D = 30$, indicating a negative effectiveness value. This may happen when the angle of incidence to the block is smaller than the initial yaw angle due to the rod rotation to the reverse direction. Penetration processes for the case of $V_p = 1.5$ km/s and $L/D = 15$ are demonstrated in Fig. 4. The rod begins to penetrate the witness block at 200 μs. At this time, the angle of incidence decreases to

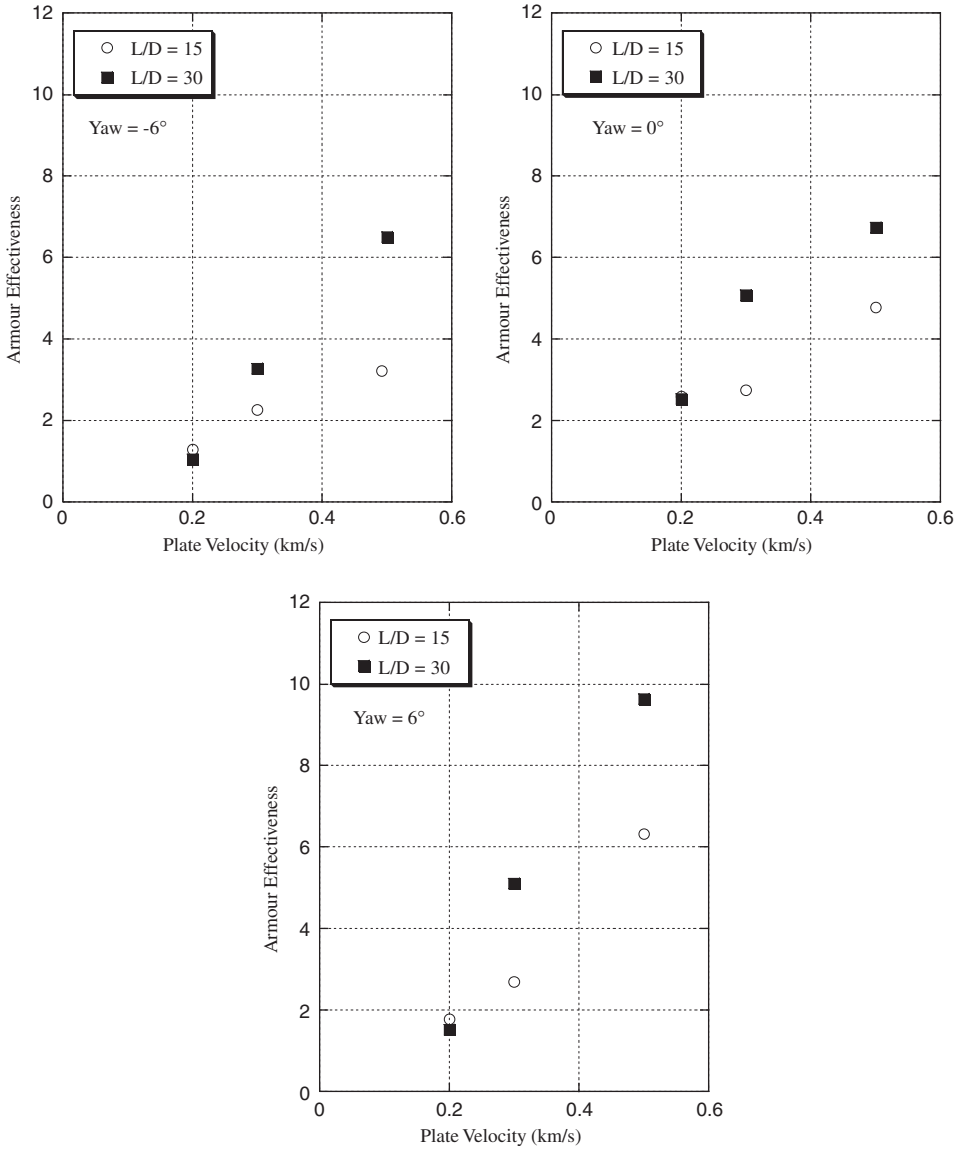

Fig. 2. Effect of plate velocity and L/D on armor effectiveness, $V_p = 2.5\,\mathrm{km/s}$.

-4.5° for $\alpha = -6^\circ$. For the case of $\alpha = +6^\circ$, even though the rod deflects when it exits the plate, it is observed that the angle of incidence of the head portion is nearly close to 90°. Larger P_{res} than P_{ref} means that this effect is greater than the other disturbance such as erosion and decrease of rod velocity.

Another tendency observed from Fig. 3 is that the armor effectiveness of positive 6° yaw is slightly higher than that of negative -6° yaw. To get a better insight of this result, the penetration processes for each case are demonstrated in Figs. 4–7. From the deformation and the size of plate holes, it is found that the negative yaw rod interacts more with the front plate than the rear plate while the positive yaw rod interacts more with the rear plate. Comparing these results, the rod of positive yaw interacting with the rear plate can be seen to be more severely damaged. A similar result is obtained for the impact of $V_{\mathrm{pl}} = 0.3\,\mathrm{km/s}$.

Now, let us consider the armor effectiveness in terms of the impact velocity from Fig. 3(a) and (b). The deviation of effectiveness is shown to be small for higher impact velocity. This is due to the enhanced kinetic energy of the rod and relatively shorter interaction time with the flying plates. We can see more severe disturbance for the rod with low impact velocity as shown in Figs. 4–7.

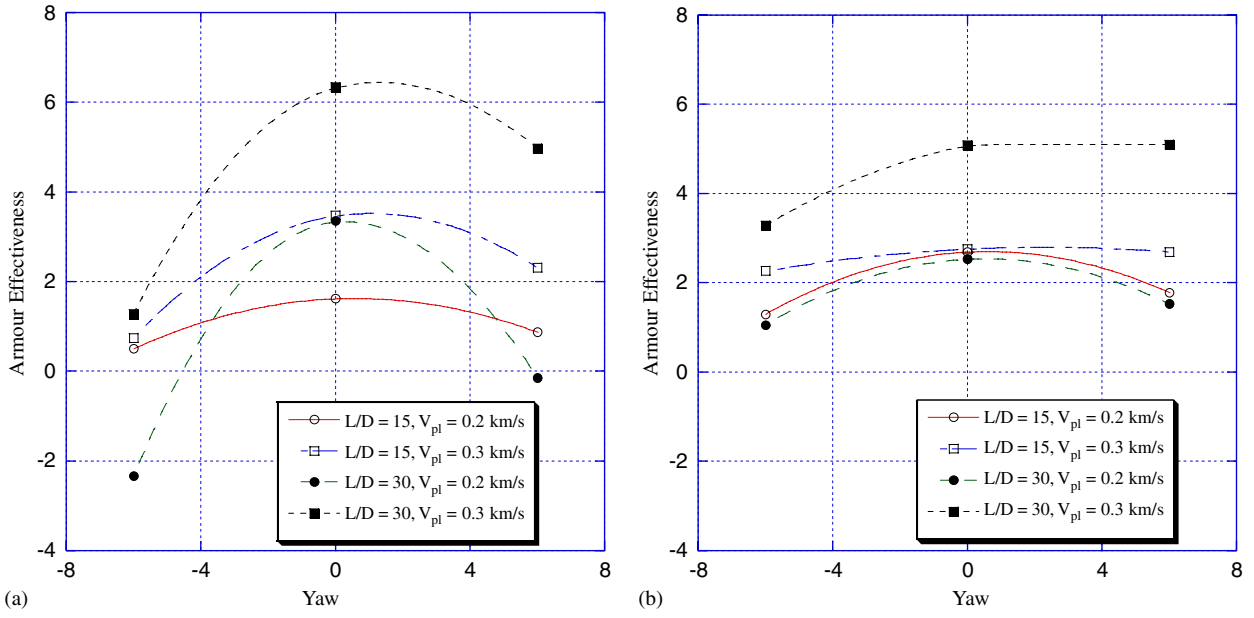

Fig. 3. Effect of yaw on armor effectiveness: (a) $V_p = 1.5\,\text{km/s}$, and (b) $V_p = 2.5\,\text{km/s}$.

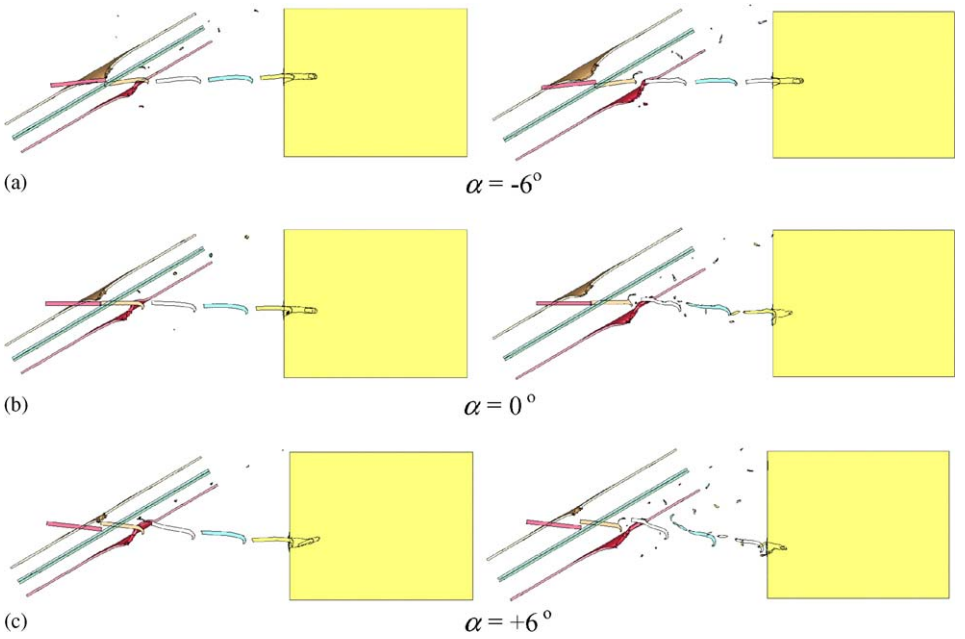

Fig. 4. Penetration process, $V_p = 1.5\,\text{km/s}$, $L/D = 15$, $V_{pl} = 0.2\,\text{km/s}$ (left), 0.3 km/s (right). Plotting time—penetrator: 0, 50, 100, 150, 200, 250, 300 μs; plate: 0, 100 μs.

The additional result supported by Figs. 2 and 3 is that flying plates are less effective against higher velocity rods. This can be shown by considering the data for $L/D = 15$ of zero yaw at 1.5 and 2.5 km/s for plate velocities of 0.2, 0.3, and 0.5. The ratios of effectiveness for the two velocities are 1.8/2.6, 3.7/2.7, and infinity/4.8.

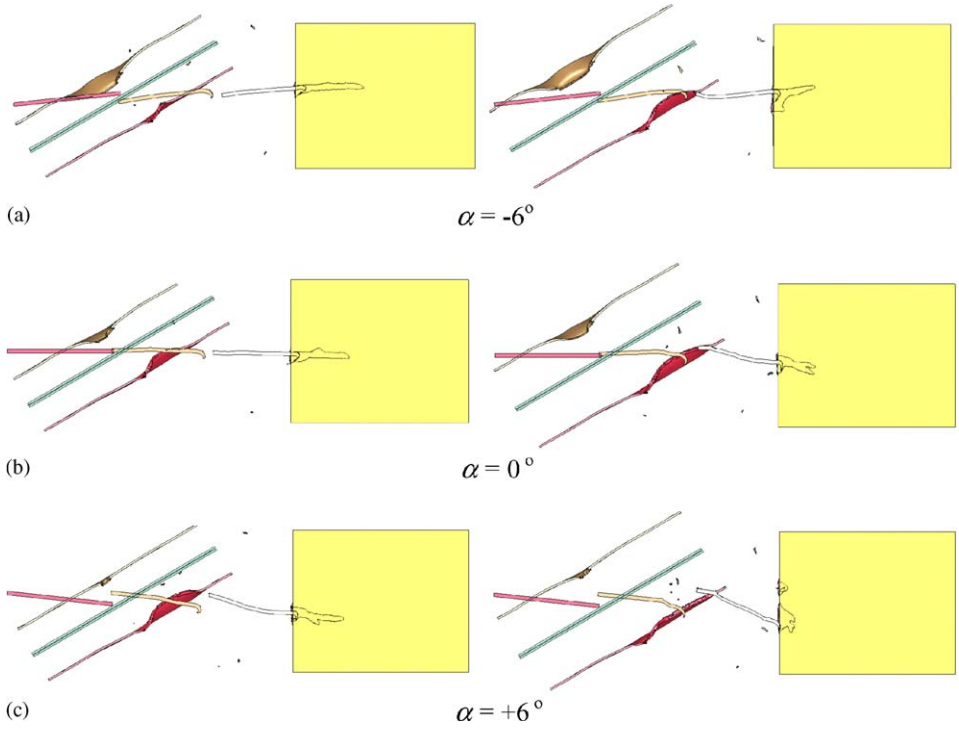

Fig. 5. Penetration process, $V_p = 1.5$ km/s, $L/D = 30$, $V_{pl} = 0.2$ km/s(left), 0.3 km/s (right). Plotting time—penetrator: 0, 100, 200, 400 μs; plate: 0, 200 μs.

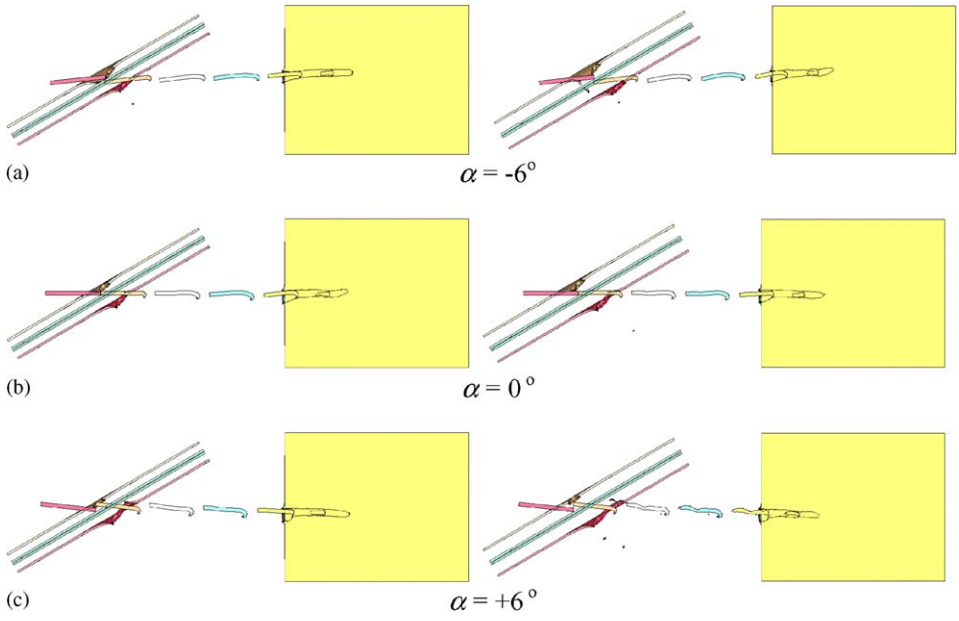

Fig. 6. Penetration process, $V_p = 2.5$ km/s, $L/D = 15$, $V_{pl} = 0.2$ km/s(left), 0.3 km/s(right). Plotting time—penetrator: 0,30, 60, 90,120,150, 200 μs; plate: 0, 60 μs.

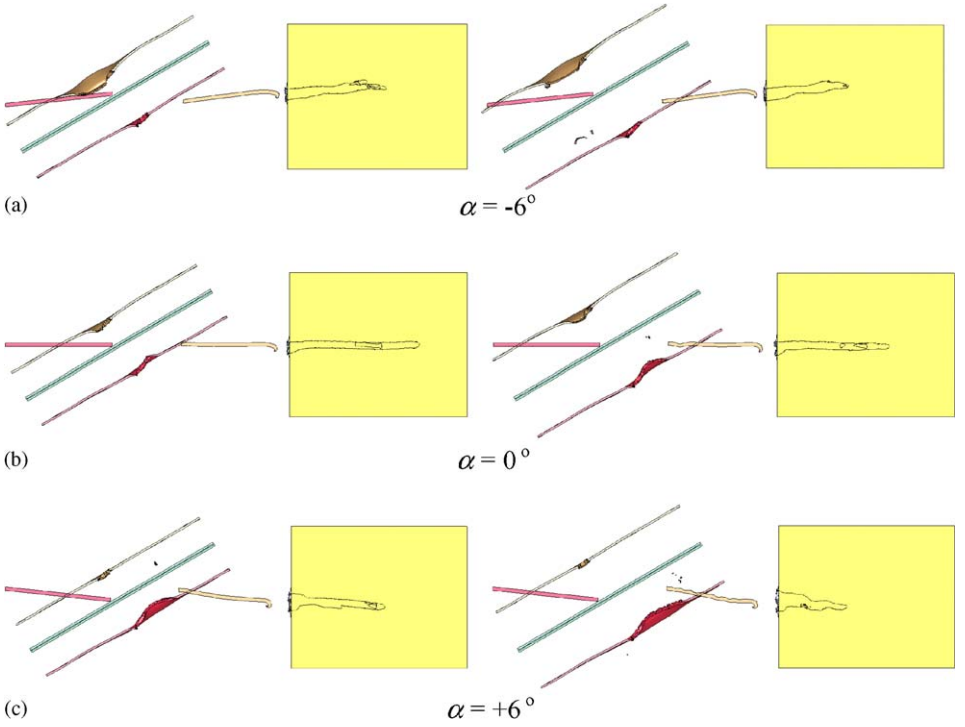

Fig. 7. Penetration process, $V_p = 2.5$ km/s, $L/D = 30$, $V_{pl} = 0.2$ km/s(left), 0.3 km/s(right). Plotting time—penetrator: 0, 100, 200, 300 μs; plate: 0, 200 μs.

4. Conclusions

Under the motivation that dual flying plates can protect a longer rod more effectively, their protection capabilities against an enhanced long rod ($L/D = 30$) with an angle of yaw was investigated numerically and compared with that of a shorter one ($L/D = 15$). In addition, the details of the interactions between a yawed long rod and dual flying plates were examined. With respect to the measure of armor effectiveness, the reference depth of penetration was estimated with the yaw impact. From the simulation, we were able to make the following conclusions.

- Dual flying plates system is more effective for an enhanced L/D rod, except for the case of $V_{pl} = 0.2$ km/s in which negligible difference between $L/D = 15$ and 30 is shown.
- Larger L/D is appeared to be more sensitive to the plate velocity.
- The armor effectiveness with respect to the angle of yaw is of convex shape and is the highest at zero yaw. This is only true if the reference DOP P_{ref} is evaluated for the direct impact into the witness block with yaw.
- Dual flying plate system is more effective for a positive yaw rod than a negative yaw rod.
- The deviation of armor effectiveness is smaller for hypervelocity impact than ordnance velocity impact.
- Flying plates are less effective against higher velocity rods.

Appendix. Verification of the code

The code (IPSAP/Explicit) verification has been carried out by comparing the prediction results with the published experimental data. A long rod impact into an oblique steel plate was chosen for this study. The diameter and length of the rod was 5 and 75 mm, respectively, resulting in L/D of 15. At 2.5 km/s, the thicknesses were 9 mm for 60° plate and 3.13 mm for 80° plate. At 1.5 km/s, the thickness of the 60° plate was 5 mm and that of the 80° plate was 1.74 mm. The material behavior was modeled with Johnson–Cook

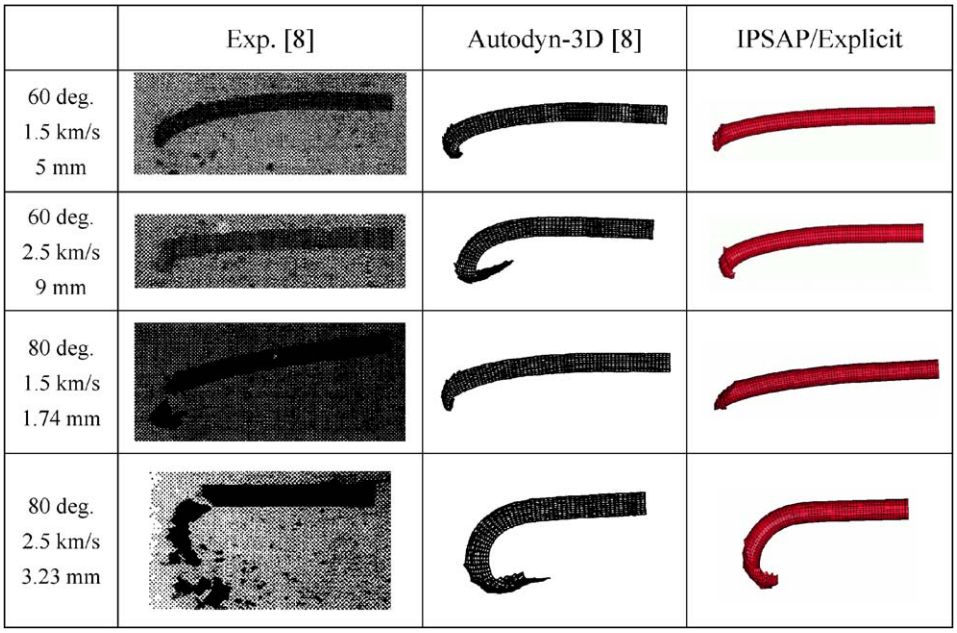

Fig. 8. Comparison of deformed shape of residual projectile.

Table 3
Comparison of simulated residual length and velocity with experiment

Oblique angle (deg.)	V_0 (km/s)	Plate thickness (mm)	Residual length (L/L_0)			Residual velocity (V/V_0)		
			Exp	Autodyn	IPSAP	Exp	Autodyn	IPSAP
60	1.5	5.0	0.85	0.87	0.84	0.97	0.98	0.98
	2.5	9.0	0.76	0.75	0.75	0.99	0.99	0.99
80	1.5	1.74	0.84	0.85	0.84	0.97	0.97	0.98
	2.5	3.23	0.62	0.68	0.63	0.98	0.98	0.99

viscoplastic model. The material for steel plate was SIS 2541-03 and that for tungsten heavy alloy was DX2HCMF. Residual deformed shapes of projectiles obtained from simulations and experiments are compared in Fig. 8. Residual lengths and velocities are shown in Table 3. The current simulation shows good agreement with the experimental data and the Autodyn-3D results [8].

References

[1] Held M, Mayseles M, Rototaev E. Explosive reactive armour. In: Proceedings of the 17th international symposium on ballistics. Midrand, South Africa, 1998. p. 33–46.
[2] Held M. disturbance of shaped charge jets by bulging armour. Propell Explos Pyrot 2001;26:191–5.
[3] Yadav HS, Kamat PV. Effect of moving plate on jet-penetration. Propell Explos Pyrot 1989;14:12–8.
[4] Normandia MJ. Eroded length model for yawed penetrators impacting finite thickness targets at normal and oblique incidence. Int J Impact Eng 1999;23(1):663–74.
[5] Bless SJ, Satapathy S, Normandia MJ. Transverse loads on a yawed projectile. Int J Impact Eng 1999;23(1):77–86.
[6] Lee M. A numerical comparison of the ballistic performance of unitary rod and segmented-rods against stationary and moving oblique plates. Int J Impact Eng 2001;26(1–10):399–407.
[7] Liden E, Johansson B, Lundberg B. Effect of thin oblique moving plates on long rod projectiles: a reverse impact study. Int J Impact Eng 2006;32(10):1696–720.

[8] Liden E, Ottosson J, Holmberg L. WHA long rods penetrating stationary and moving oblique steel plates. In: Proceedings of the 16th international symposium on ballistics. San Francisco, USA, 1996. p.703–11.
[9] Shin H, Yoo Y- H. Effect of the velocity of a single flying plate on the protection capability against obliquely impacting long rod penetrators. Combust Explo Shock Wave 2003;39:591–600.
[10] Yoo Y- H, Shin H. Protection capability of dual flying plates against obliquely impacting long rod penetrators. Int J Impact Eng 2004;30:55–68.
[11] Paik SH, Moon JJ, Kim SJ, Lee M. Parallel performance of large scale impact simulations on linux cluster super computer. Comput Struct 2006;84(10–11):732–41.
[12] Flanagan DP, Belytschko T. A uniform strain hexahedron and quadrilateral and orthogonal hourglass control. Int J Numer Meth Eng 1981;17:679–706.
[13] Benson BJ, Hallquist JO. A single surface contact algorithm for the post buckling analysis of structures. Comput Methods Appl Mech Eng 1990;78:141–63.
[14] Heinstein MW, Mello FJ, Attaway SW, Laursen TA. Contact-impact modeling in explicit transient dynamics. Comput Methods Appl Mech Engrg 2000;187:621–40.
[15] Goudreau GL, Hallquist JO. Recent developments in large-scale finite element Lagrangian Hydrocode technology. Comp Methods Appl Mech Eng 1982;33(1–3):725–57.
[16] Johnson GR, Cook WH. A constitutive model and data for metals subjected to large strains, high strain rated, and high temperatures. In: Proceedings of the 17th international symposium on ballistics. Hague, Netherlands, 1983. p. 541–47.
[17] Fugelso E, Taylor JW. Evaluation of combined obliquity and yaw for U 0.75 wt% Ti penetrators. Los Alamos Scientific Laboratory, LA-7402-MS, 1978.
[18] Cagliostro DJ, Mandell DA, Schwalbe LA, Adams TF, Chapyak EJ. MESA 3-D calculations of armor penetration by projectiles with combined obliquity and yaw. Int J Impact Eng 1990;10:81–92.
[19] Anderson Jr CE, Walker JD, Bless SJ, Partom Y. On the L/D effect for long-rod penetrators. Int J Impact Eng 1996;18:247–64.
[20] Anderson Jr CE, Walker JD, Bless SJ. On the velocity dependence of the L/D effect for long-rod penetrators. Int J Impact Eng 1995;17:13–24.
[21] Gee DJ, Littlefield DL. Yaw impact of rod projectiles. Int J Impact Eng 2001;26:211–20.